J Musculoskel Neuron Interact 2003; 3(4):418-430

Hylonome

Poster abstracts from the 33rd Meeting of the International Sun Valley Hard Tissue Workshop

3-7 August 2003, Sun Valley, Idaho, USA

Program Chairmen: Webster S.S. Jee and David B. Burr

Abstract No.	Topic
P1-28	Poster abstracts (Authors marked with an asterisk (*) are Young Investigator Travel Awardees)

P-1

Practical Issues in X-Ray Microtomographic Imaging of Mouse Bone

*D.J. Adams, V. Diaz-Doran, M.S. Moreau
Dept. of Orthopaedic Surgery, University of Connecticut Health Center, Farmington, CT, USA
E-mail: dadams@nso.uchc.edu

The use of computed microtomography (μCT) for imaging and quantitating skeletal architecture in mice is quickly becoming a standard laboratory tool. The current maximum spatial resolution of commercially available imaging systems is approximately 10 μm, while the thickness and spacing of trabeculae in mouse bone typically range from 70 μm down to 20 μm and smaller. Meaningful quantitation of mouse trabecular bone architecture is dependent on this potential limitation imposed by image accuracy, as well as the variation associated with inherent stochasticity of the imaging instrument and its operation. The practical utility of designing experiments using mice also is affected by the degree of biologic variation between animals, which varies by mouse strain. Moreover, phenotypic differences associated with different strains of mice that are exploited in experimental design can depend on the skeletal site examined and can exhibit sexual dimorphism.

To manage these confounding issues at the resolution level of mouse skeletal architecture, this study formally examined the baseline precision in measuring mouse bone trabecular architecture using state-of-the-art μCT instrumentation. Instrument and operator precision were assessed by repeated three-dimensional imaging and measurement of mouse bone morphometry using commercially available fanbeam and conebeam X-ray computed microtomography instruments with a 7 μm focal spot (models μCT20 and μCT40, Scanco Medical, Bassersdorf, Switzerland). Sensitivity of morphometric measurements to spatial resolution was evaluated by permuting discrete voxel density. Sensitivity to X-ray exposure was evaluated by permuting integration time at each discrete projection. Bones from 4-month-old inbred strains of mice typically associated with low (C57Bl/6) and high (C3H/He) bone density, as well as the outbred CD1, were imaged and quantified to elucidate biologic variation as well as gender-, site, and compartment- specific (cortical versus trabecular) differences in morphometry.

Instrument precision obtained by repeated measurements of mouse vertebrae (exhibiting relatively high bone volume fraction) demonstrated variation less than 3% for nearly all morphometric parameters and typically less than 1%. In femurs with relatively low bone volume fraction, however, instrument precision demonstrated larger variation which was particularly problematic in discriminating trabecular connectivity. Precision generally increased with voxel density, reflecting significant ($p < 0.01$) relative changes in morphometric parameter magnitudes associated with partial volume artifact. Increasing exposure time per projection beyond a modest level demonstrated no significant effect on precision, with morphometric parameter magnitudes changing less than 4%. Precision associated with routine variation in operation of the imaging instruments, including placing samples and selecting regions of interest, demonstrated variation in morphometric measurements less than 5%, a value exceeding instrument precision but significantly less than the variation incurred for strain-, age-, and gender-matched animals, which can exceed 30%.

Trabecular volume fraction was significantly lower ($p = 0.004$) in femora from B6 females than in B6 males (10.7 ± 0.8% vs. 28.1 ± 8.4%), and significantly higher ($p = 0.01$) in C3H females than in C3H males (33.5 ± 4.2% vs. 21.8 ± 7.4%). Femoral trabeculae in B6 females were thinner ($p = 0.008$), fewer in number ($p = 0.002$), and less connected ($p = 0.006$) than in males, whereas the trabeculae in C3H females were significantly thicker than in males ($p = 0.03$). Cortical cross-sectional area, thickness, maximum area moment of inertia, and polar moment of inertia were significantly lower in femora from females than in males for B6 and CD1 mice ($p < 0.05$), but not for C3H mice. Flexural section modulus, a measure of structural bending strength due to cross-sectional size and shape, was lower in females than in males for all three strains ($p < 0.05$), although only marginally significant for CD1 ($p = 0.057$). Despite substantial differences in cortical cross-sectional area and thickness, section modulus was the same in female C3H and B6 femora; however, section modulus was significantly lower in B6 males than C3H males ($p = 0.04$).

Unlike the aforementioned differences in cortical bone geometry, differences in trabecular bone morphometry between male B6 and C3H mice were minimal, including a small increase in the number of trabeculae ($p = 0.004$) that were otherwise of equal average thickness and not consequential in altering volume fraction ($p = 0.2$). Trabecular number, thickness, connectivity, and volume were substantially lower in B6 females than C3H females ($p < 0.005$).

These data demonstrate that phenotypic differences in bone morphometry typically associated with C3H and B6 mice are gender and site specific. Because the female mice of these two inbred strains are regarded as high and low bone mass animals, the discrepancies associated with gender, site, and compartment are of particular interest in the design of studies that aim to exploit baseline differences in bone mass and architecture.

P-2

The Effects of Ovariectomy on Intracortical Remodeling in the Female Ferret (Mustela Furo): A Pilot Study

*A.B. Castillo, L.N. Metz, R.B. Martin
Orthopaedic Research Laboratories, University of California, Davis

Medical Center, Sacramento, CA, USA
E-mail: abcastillo@ucdavis.edu

Introduction: Postmenopausal osteoporosis (PMO) is a bone condition characterized by low bone mass and deterioration of bone microarchitecture resulting in increased bone fragility and fracture risk in humans[1]. The primary factor linked with the onset of PMO is reduced estrogen levels during the postmenopausal period, which results in increased bone remodeling and bone loss. Microdamage and removal of microdamage, which involves initiation of remodeling and increased remodeling space, are also proposed to play a role in postmenopausal bone fragility[2]. While approximately 46% of osteoporotic fractures are vertebral fractures and, thus, associated mostly with cancellous bone, one cannot presently study the initiation of remodeling in this tissue[3]. This is because individual basic multicellular units (BMU) are harder to identify in trabecular bone than in cortical bone. Therefore, the study of the roles of both estrogen loss-induced and microdamage-induced remodeling in such fractures will begin in a normally remodeling cortical bone model. Rats do not normally undergo cortical remodeling and, thus, cannot be used. Dogs do exhibit cortical remodeling; however, they are relatively large and costly to house and maintain. The ferret is an attractive alternative because it undergoes osteonal remodeling of its cortical bone and is a relatively small animal. In addition, the ferret exhibits a significant decrease in trabecular bone mass in the proximal tibia following ovariectomy[4,5]; however, the effects of ovariectomy on cortical bone remodeling remain unstudied in this animal. The purpose of this experiment was to assess the appropriateness of the ferret as a cortical bone model for studying intracortical remodeling and changes in bone mechanical properties following ovariectomy. To do this we answered the following specific questions: (1) does ovariectomy result in a significant increased intracortical remodeling in the ferret ulna and (2) are mechanical properties of the femur was significantly reduced following ovariectomy?

Methods: Eight intact and eight ovariectomized (ovx) female ferrets (*Mustela furo*), 9 months of age, were housed individually under a 16h:8h light/dark photoperiod. The day of ovariectomy was designated as day 0 of the study. Blood samples were collected on days 20 and 45 and assayed for estradiol. *In vivo* bone labels were administered IP at 10 and 3 days pre-euthanasia. All animals were euthanized on day 45. Histomorphometric analysis of the entire ulnar cortical diaphysis was performed[6-8]. The left and right whole femora were monotonically tested to failure in three-point bending. Bone structural and tissue properties were calculated using beam theory. Data were checked for normality and constancy of variance. When these assumptions were not met, the data were transformed. Data were analyzed using a one-way ANOVA with animal condition (intact vs. ovx) as the main factor. Alpha (α) = 0.05 for all statistical tests.

Essential results: One intact ferret was excluded from the study because it had a severe kidney infection. All intact ferrets went into estrus during the study period. Serum estradiol concentration was approximately 60% lower in ovx ferrets than in intact estrous ferrets at day 45 ($p<0.001$). Resorption cavity density (rCv.Dn) was 3.2-fold greater, activation frequency (Ac.f) was 4.4-fold greater, and bone formation rate (BFR) was 7.8-fold greater in ovx ferrets than in intact ferrets (Figures 1-3). There were no significant differences in femoral mechanical properties between the two groups.

Discussion: The ferret undergoes intracortical remodeling as evidenced by the presence of secondary osteons in their long bone cortices. While the level of baseline intracortical remodeling in the ulna is low, our results indicate remodeling significantly increases in response to ovariectomy. This remodeling response is similar to the response seen in monkey humeri and dog rib cortical

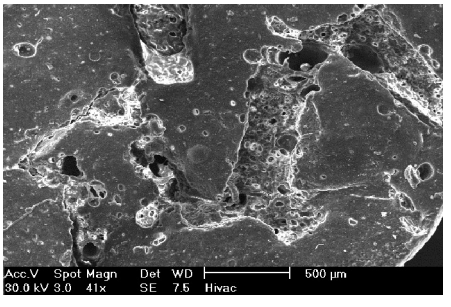

Figure 1. SEM of composite polymer. (P3)

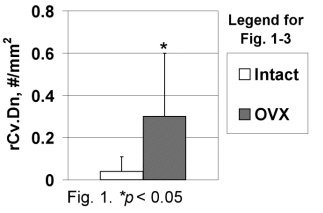

Fig. 1. *$p < 0.05$

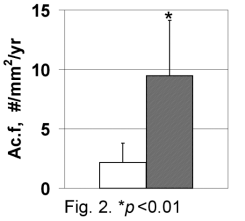

Fig. 2. *$p<0.01$

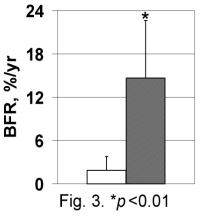

Fig. 3. *$p<0.01$

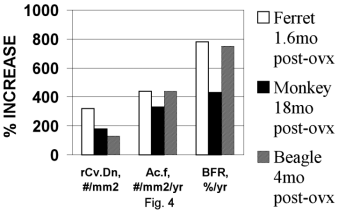

Fig. 4

bone (Figure 4) following ovariectomy[9,10]. An intracortical remodeling response to ovariectomy is not seen to any great degree in the rat[11]. Mechanical properties of the femur in ovx ferrets were not significantly reduced at 45 days. Greater differences in femoral mechanical properties may have developed with a longer study period. Assessment of more clinically relevant sites will be examined in future experiments. The ferret may be a suitable cortical bone model for studying the intracortical remodeling response to reduced estrogen levels because (1) it has normally remodeling cortical bone, albeit at a slow rate, (2) intracortical remodeling increases significantly within 45 days following ovariectomy and (3) it is a relatively small animal that is less expensive to house and maintain than larger animals. One caution when using the ferret model is that it has relatively small bones, and only a small amount of bone material is available for examination. Thus, it is necessary to examine the entire diaphysis of one or many bones from each animal, or examine several animals, to get accurate baseline histomorphometric data. A second caution is intact females will go into estrus and remain in estrus until bred or until treated with gonadotropin hormone. Females in protracted estrous (6-8 weeks) can develop bone marrow depression, which is usually fatal when left untreated[12].

References

1. National Institutes of Health. Osteoporosis prevention, diagnosis, and therapy. JAMA 2001; 285:785-795.
2. Burr DB, Forwood MR, Fyhrie DP, Martin RB, Schaffler MB, Turner CH. Bone microdamage and skeletal fragility in osteoporotic and stress fractures. J Bone Miner Res 1997; 12:6-15.
3. National Osteoporosis Foundation. Electronic Source: nof.org/osteoporosis/stats.htm. 2002.
4. Gropp K, Mackey M, Phipps R, Smith P. Short-light cycle or GnRH increases bone turnover in female ferrets. 34th Annual Meeting of the American College of Veterinary Pathologists, Albuquerque, New Mexico; 1997:488.
5. Mackey MS, Stevens ML, Ebert DC, Tressler DL, Combs KS, Lowry CK, Smith PN, McOsker JE. The ferret as a small animal model with BMU-based remodeling for skeletal research. Bone 1995; 17:191S-196S.
6. Burr DB, Hooser M. Alterations to the en bloc basic fuchsin staining protocol for the demonstration of microdamage produced *in vivo*. Bone 1995; 17:431-433.
7. Martin RB, Burr DB, Sharkey NA. Skeletal Tissue Mechanics. Springer-Verlag, New York; 1998:88-93.
8. Parfitt AM, Drezner MK, Glorieux FH, Kanis JA, Malluche H, Meunier J, Ott SM, Recker RR. Bone histomorphometry: standardization of nomenclature, symbols, and units. Report of the ASBMR Histomorphometry Nomenclature Committee. J Bone Miner Res 1987; 2:595-610.

9. Burr DB, Hirano T, Turner CH, Hotchkiss C, Brommage R, Hock JM. Intermittently administered human parathyroid hormone(1-34) treatment increases intracortical bone turnover and porosity without reducing bone strength in the humerus of ovariectomized cynomolgus monkeys. J Bone Miner Res 2001; 16:157-165.
10. Wilson AK, Bhattacharyya MH, Miller S, Mani A, Sacco-Gibson N. Ovariectomy-induced changes in aged beagles: histomorphometry of rib cortical bone. Calcif Tissue Int 1998; 62:237-243.
11. Kalu DN. Evaluation of the pathogenesis of skeletal changes in ovariectomized rats. Bone Miner 1991; 115:507-512.
12. Bernard SL, Leathers CW, Brobst DF, Gorham JR. Estrogen-induced bone marrow depression in ferrets. Am J Vet Res 1983; 44:657-661.

P-3

Alternative Therapies for Senile Osteoporosis: Morphological Study Using Murine Model

*H. Chen[1], S. Shoumura[1], H. Isono[2], C. Ai[3]
[1] Department of Anatomy, Gifu University School of Medicine,
[2] Heisei College of Medical Technology, Gifu, Japan,
[3] Qinghai Jinhe Tibetan Medicine Consortium Ltd., Xining, China
E-mail: huayue@cc.gifu-u.ac.jp

The alternative therapy for senile osteoporosis with traditional Chinese medicine or Tibetan medicine was practiced using the murine model (SAMP6). We investigated the bone and the calcium-regulating organs morphologically after treatment with these medicines. The levels of serum Ca, PTH, calcitonin, E2 levels and the bone mineral density (BMD) were also studied.

Two-month-old SAMR1 (a normal strain of mice) and SAMP6 mice were divided into control and experimental groups. The control animals took the tap water freely. The experimental mice were given 0.05% solution of the traditional Chinese medicine, Ba-Wei-Di-Huang-Wan (Tsumura & Co., Japan) or 0.03% solution of the Tibetan medicine (Qinghai Jinhe Tibetan Medicine Consortium Ltd., China) as the only drinking fluid available. Three months later, the serum Ca, P, PTH, calcitonin and E2 levels were measured. The BMD of the whole body was determined by DEXA method. The femurs, tibias, lumbar vertebrae, thyroid and parathyroid glands were processed for microscopic examination.

There was no marked difference between the control and experimental SAMR1 mice regarding the morphology of the bones and parathyroid glands. As compared with SAMR1 mice, the BMD and the bone mass was significantly reduced in control SAMP6 mice. The number of the osteoblasts in trabecular bones significantly decreased, the serum PTH level increased and the serum E2 level decreased in control SAMP6 mice. The osteocytes and osteoblasts showed morphologically degenerative changes, the mast cell number in the bone marrow and the periosteum of the femur significantly increased in control SAMP6 mice.

After treatment with the traditional Chinese medicine or the Tibetan medicine, the bone mass and the percentage area occupied by the forming surface increased. The degenerative changes of the osteocytes and the osteoblasts were reduced in SAMP6 mice. The number of mast cells in the bone marrow and the periosteum decreased after treatment with the traditional Chinese medicine. While the serum PTH level decreased after treatment with the Tibetan medicine.

These data suggest that the bone loss in SAMP6 mice can be significantly reduced by administration with traditional Chinese medicine, Ba-Wei-Di-Huang-Wan, or Tibetan medicine.

P-4

Response to Drug and Exercise Intervention Depends on Initial Bone Mass and Density

S. Cheng, S. Sipilä, H. Sievänen, A. Heinonen, K. Uusi-Rasi, D.R. Taaffe, P. Nicholson, J. Puolakka , J. Timonen, P. Kannus, H. Suominen
University of Jyväskylä, Jyväskylä and UKK Research Institute, Tampere, Finland
E-mail: sulin.cheng@sport.jyu.fi

In most hormonal and anti-resorptive therapy or exercise intervention trials

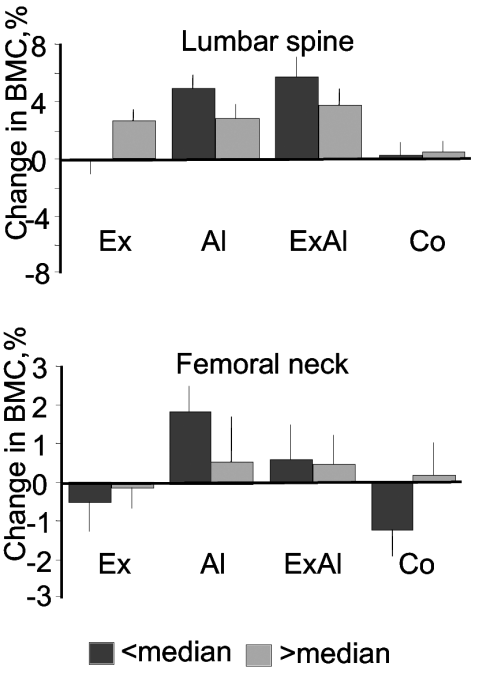

to date, the possible influence of the subjects' initial bone mineral content (BMC) and density (BMD) values has not been considered. To test whether the response to drug and exercise intervention depends on the initial BMC and BMD at different bone sites, we divided the subjects into two groups on the basis of their baseline BMC/BMD level (< median and >median) in two one-year randomized controlled trials [estrogen (Es) + exercise (Ex), and alendronate (Al) + Ex] in early postmenopausal women (age range from 48 to 59). When compared to non-exercised placebo controls (Co), those women in the Al and AlEx groups with low initial values increased their BMC (DXA) in the lumbar spine and femoral neck (see Fig.) and BUA (QUS-2) in the calcaneus more than those with high initial values. The changes in the Ex group were less evident and not systematically related to the baseline values. Neither were the changes in the ExEs trial significantly associated with the initial BMD values (QCT, SPA), although there was an overall increase in BMD at the proximal femur and tibia, tibial shaft and calcaneus in the Es and EsEx groups, and at the tibia and calcaneus in the Ex group. The results indicate that the response of bone mass and density to anti-resorptive alendronate therapy in early menopause is higher in women with low initial BMC in trabecular bone sites. Hormone replacement therapy is likely to be effective in most bone sites and high impact exercise in distal bone sites of the lower limb; however, the responses are not consistently related to initial BMD. These are important findings in terms of developing strategies for targeting interventions to combat osteoporosis in those subjects most likely to benefit.

P-5

Effects of Bipedal Loading During Lactation and Post-Lactation Recovery on Femoral Bone Strength in Rats

*S.L. Doody[1,2], J.E. Shea[2], P.A. Eisenman[1], S.C. Miller[2,1]
[1] Department of Exercise and Sport Science, College of Health,
[2] Radiobiology Division, School of Medicine, University of Utah, Salt Lake City, UT
E-mail: s.doody@m.cc.utah.edu

Introduction: During lactation, there are significant decreases in bone mass in both cortical and cancellous sites to provide calcium for milk production. Following lactation, there is a recovery period, resulting in increases in bone formation and accumulation of bone mass, as well as improvements in bone strength. Mechanical loading in the form of bipedal loading has also been shown to be anabolic to the skeleton. Therefore, the primary aim of this study was to determine if the post-lactation recovery period and bipedal loading could provide additive and synergistic effects on

femoral bone strength. A secondary aim of this study was to determine if bipedal loading during lactation could mitigate bone loss at the femur.

Methods: Nulliparous female rats (90-100 days old; N = 32) were permitted to go through two reproductive cycles. After the second parturition, rats were randomized into four groups: (1) Lactation (L; n = 8); (2) Lactation, Raised Cage (L RC; n = 8); (3) Lactation, Recovery (LR; n = 8) and; (4) Lactation, Recovery, Raised Cage (LR RC; n = 8). After 21-days of lactation, the L and L RC were necropsied and the LR and LR RC continued on for an additional six weeks to assess the recovery period. The right femurs were excised at necropsy and scanned using a portable, peripheral dual energy x-ray absorptiometer (pDXA) to determine mid-diaphyseal and whole femoral bone mineral density (BMD, g/cm^2) and bone mineral content (BMC, g). The mechanical properties (peak load, break load, slope, and energy to peak fracture) of the mid-shaft of the right femur was determined by three-point bending using a materials testing machine (MTS) with a 5 kN load cell. Each femur was loaded to failure at the mid-diaphysis at a rate of 10 mm/min with displacement measured by cross-head movement.

Results: There were no differences in whole bone or mid-shaft femoral BMD and BMC between L and L RC. L had greater peak load ($p < 0.02$) and break load ($p < 0.02$) than L RC, with no differences in slope or energy to fracture. LR RC had greater whole femoral BMD ($p < 0.01$) than LR, with a trend in BMC ($p < 0.07$). There were no differences in mid-shaft femoral BMD, BMC, peak load, break load, slope, or energy between LR and LR RC. LR and LR RC had greater whole femoral BMD ($p < 0.0001$) and BMC ($p < 0.0001$) than L and L RC. LR and LR RC also had greater cortical mid-shaft BMD than L RC ($p < 0.001$) and no difference in BMC. LR RC had greater peak load ($p < 0.02$) and slope ($p = 0.05$) than L RC with no differences in break load or energy to fracture.

Discussion: There was no loading effect during lactation, possibly because Ca^{2+} needs for milk production have greater physiological priority than adaptations to loading. There was an additive and synergistic effect between bipedal loading and post-lactation recovery on whole femoral BMD and BMC, but differences in BMD, BMC, and mechanical properties were not significant at the cortical mid-shaft. These data suggest that loading had a greater effect at cancellous sites.

P-6

Biomechanical Impact of Aluminum Accumulation on Rat Cortical Bone

G.R. Cointry[1], A.L. Negri[2], J.L. Ferretti[1]
[1] Center for P-Ca Metabolism Studies (CEMFoC), Faculty of Medicine, National University of Rosario, Argentina,
[2] Research Department, Del Salvador University, Buenos Aires, Argentina
E-mail: ferretti@idim.com.ar, jlferretti@arnet.com.ar

In order to analyze the biomechanical impact of a chronic aluminum accumulation in bone tissue on the whole-bone behavior, 14 rats aged 90 days received ip doses of 27 mg/d of elemental Al as Al(OH)3 during 26 weeks while another 14 remained as controls. Their femur diaphyses were studied tomographically (pQCT) and mechanically tested in bending. The load/deformation curves obtained allowed a distinction between effects observed during the linearly elastic (Hookean) and non-linear (non-Hookean) behaviors of bones before and after the yield point, respectively.

No effects on body weight were observed. Aluminemia and bone histological data confirmed the Al accumulation. Treatment reduced the cortical bone mineralization (volumetric cortical BMD, $p<0.01$) with a negative impact on the intrinsic bending stiffness of the cortical tissue (calculated Young's elastic modulus, $p<0.05$). Despite the absence of any cortical mass increase (cortical cross-sectional area), an improvement of the distribution of the available cortical tissue in space (cortical cross-sectional moment of inertia for A-P bending, $p<0.05$) occurred through a directional modulation of the modeling drifts during growth.

This presumably adaptive response should have proved adequate for maintaining a normal diaphyseal stiffness (load/deformation ratio) according to the bone "mechanostat" theory, but not so as to provide a complete neutralization of the impaired diaphyseal strength (ultimate load reduction, $p<0.05$). Although a relative inhibition of bone formation could not be discarded, an Al-induced impairment of the bone ability to resist loads beyond the yield point (difference between the ultimate and yield loads, $p<0.01$) should have caused the striking disruption observed between effects on bone stiffness and strength.

In addition to describing an unusual finding, these results suggest that the little-known microstructural factors affecting the post-yield behavior of cortical bone in these and other conditions ought to be further investigated in specifically designed studies as a novel, promising field in skeletal research.

P-7

Effects of Hypophysectomy and Recombinant Human Growth Hormone on Rat Femur Diaphyses and Gastrocnemius Muscles

G. Cointry, S. Feldman, R Capozza, L. Sarrió, J.L. Ferretti
Center for P-Ca Metabolism Studies (CEMFoC) and Dept of Physiology, Faculty of Medicine, National Univ of Rosario; BioSidus Labs, Buenos Aires, Argentina
E-mail: ferretti@idim.com.ar, jlferretti@arnet.com.ar

Aiming to analyze biomechanically the musculoskeletal effects of Hx and a partial replacement with rhGH, we determined the intrinsic stiffness (elastic modulus, E) and volumetric BMD (vBMD) of the cortical bone; the area and moment of inertia (CSMI) of the cross-sections, and the structural stiffness and pre- and post-yield strength of the femur diaphyses (by pQCT and mechanical tests), and the gastrocnemius weight of rats (Charles Rivers Labs, USA), either intact (n = 9) or hypophysectomized (Hx) at 15 days of age (20), otherwise untreated (Hx controls, 4) or given 30 (8) or 150 (8) mIU/d sc of recombinant human growth hormone (rhGH) 15 days post-surgery for 45 days.

The Hx delayed the bone / muscle development (gastrocnemius weight, bone geometric properties) with no complete catch-up, thus affecting the diaphyseal stiffness and strength. It also reduced the cortical vBMD through an undefined mechanism, paradoxically increasing the elastic modulus of cortical bone. The Hx also affected the correlation between bone geometric and material properties CSMI vs. E), suggesting an anti-anabolic shift of the bone mechanostat setpoint for triggering the one modeling response to strains provoked by mechanical usage, that was partially prevented by hGH. As an integrated result, Hx reduced the stiffness and the post-yield and ultimate strength of the diaphyses. The rhGH treatment tended significantly to prevent Hx effects on bone and muscle development correlatively; but it failed to prevent the bone material stiffening (E) and the impairment in structural stiffness / strength of the diaphyses.

The Hx effects on bone/muscle development (geometry) were closely parallel as expected. Not so curious was the demineralizing / stiffening effect of Hx on bone tissue and the unusual effects observed on the post-yield strength (less clearly related than the former to muscle development and unaffected by rhGH at the assayed doses). These could reflect changes in bone tissue microstructure associated with crack generation and progress, unrelated to bone mineral mass (delay in collagen turnover with associated changes in crystal size and arrangement), resulting from the suppression of some other hormones, such as thyroid. This may explain why rhGH tended to normalize the relationship between bone geometry (but not strength) with muscle mass.

The effects of larger rhGH doses and the interaction of other hormones with the described effects remain to be investigated.

P-8

Alendronate Effects on Rat Cortical Bone May Not Entirely Depend Upon Bone Mass and Mineralization

M.A. Chiappe[1], G.R. Cointry[2], R.F. Capozza[2], G. Iorio[1], E. Alvarez[1], J.R. Zanchetta, J.L. Ferretti[2]
[1] Dept of Physiology, Faculty of Veterinary Sciences, Univ. of Buenos Aires,
[2] Center for P-Ca Metabolism Studies (CEMFoC), National Univ. of Rosario, Argentina
E-mail: ferretti@idim.com.ar, jlferretti@arnet.com.ar

In order to describe Alendronate (AL) effects on cortical bone, forty 3-month-old rats were ovariectomized (OX) and immediately given sc doses of 0 (OX ctrl, n=13), 5 (OX+5, 13), and 25 ug/kg (OX+25, 14) of AL 2/wk

during 6 months, while a further 15 remained as sham controls. Their femur diaphyses were studied by DEXA and pQCT and tested in bending.

Despite no differences in bone mineralization ("areal" or volumetric BMD) and geometry (cortical cross-sectional diameters, area, and bending moment of inertia, CSMI) were observed, the OX reduced all bone tissue stiffness (elastic modulus, E), diaphyseal stiffness, load supported at the yield point, and ultimate load. The post-yield behavior of the bones (difference between ultimate and yield loads) was strikingly improved by OX, presumably as a consequence of the inverse relationship usually observed between effects on crack generation (facilitated in this case) and progression. AL treatment prevented all negative OX effects and improved the bones' ultimate strength over sham values at the highest dose. Despite the load at the yield point was normal in AL-treated groups (no effects on crack generation), their bones showed the same improvement in the post-yield strength as those from OX rats (resistance to crack progress). The negative correlations observed between bone architecture (CSMI, y) and material quality indicators (E, x) showed significant "anti-anabolic" shifts for the OX group and "anti-catabolic" displacements for the OX+AL groups with respect to controls.

This should have reflected negative and positive interactions of OX and AL, respectively, with the feedback control of bone geometry as a function of bone material stiffness according to the mechanical usage of the skeleton (bone "mechanostat" theory). Lack of effects on mineralization and geometry and the effects on post-yield bone behavior suggest that both OX and AL treatment would have affected the microstructural determinants of bone material stiffness / strength which are unrelated to bone mineralization. Data suggest that the improvement induced in the post-yield behavior of bones by both OX and AL treatment should have reflected different effects on those factors.

These novel aspects of bisphosphonate effects, perhaps related to the observed dissociation between bisphosphonate effects on BMD and fracture incidence in clinical studies, deserve further attention.

P-9

Reference Study in 1,900 Normal Men and Pre- and Post-Menopausal Women

R.F. Capozza, C. Cure-Cure, G.R. Cointry, P. Cure-Rodríguez, J.L. Ferretti
Universidad Metropolitana de Barranquilla, Colombia, Centre for P-Ca Metabolism Studies (CEMFoC), National University of Rosario, Argentina,
E-mail: ferretti@idim.com.ar, jlferretti@arnet.com.ar

In whole-body studies with DXA [Ferretti et al; Bone 22:683,1998, n = 1,450] we had shown that the densitometric mineral mass, either crude (BMC) or statistically adjusted to fat mass (FA-BMC) in order to avoid any fat interference with its determination, correlated linearly with the lean mass (LM) showing similar slopes but decreasing intercepts in the order: pre-MP women > men > post-MP women > children. This evidenced 1. the homogeneous control of bone status by muscle strength in the species through the bone "mechanostat", and 2. the interaction of sex hormones with that regulation. Now we aim to expand that evidence by studying 1,900 normal Hispanic adults (60 men, 600 pre-menopausal women, 1,240 post-menopausal women), including also the same determinations in the upper and lower limbs.

In all the studied regions, the slopes of the BMC or FA-BMC vs. LM relationships were always parallel. However, interestingly region-related differences were found between the intercepts of the curves. In the whole body, the crude-BMC/LM relationships showed the same intercept differences as previously observed (pre-MP women > men > post-MP women). In the lower limbs the variance of the data was substantially reduced, and those differences were highly significant but lesser in magnitude, showing the order: pre-MP women > men = post-MP women. In the upper limbs the decreasing intercept order was: men > pre-MP women > post-MP women. After fat-adjustment of the BMC, the intercept order in both limbs was men > pre-MP women > post-MP women. Parallelism of the curves was maintained in all cases.

The parallelism of the curves suggests a common biomechanical control of bones by muscles in the species. Assuming that LM is proportional to muscle mass, results suggest that the sex-hormone-induced differences in the DXA-assessed muscle-bone proportionality in humans would vary according to the region studied. Assuming also that BMC adjustment reduced the influence of fat on body weight, this could be related to the different weight-bearing nature of the musculoskeletal structures studied. The study design did not account for some gender-related aspects of hand/foot skeletal morphometry which could also help to explain those differences.

P-10

Novel Differential Diagnosis of "Metabolic" Osteopenias and Related Fractures in Pre- and Post-Menopausal Women

J.L. Ferretti[1], R.F. Capozza[1], G.R. Cointry[1], P. Cure-Ramírez[2], C. Cure-Cure[2]
[1] Centre for P-Ca Metabolism Studies (CEMFoC), National University of Rosario, Argentina,
[2] Metropolitan University of Barranquilla, Colombia,
E-mail: ferretti@idim.com.ar, jlferretti@arnet.com.ar

Introduction. Standard densitometry (DEXA) can analyze some aspects of the muscle-bone relationships by assessing suitable indicators of "bone" (BMC) and "muscle" (lean, LM) masses. The z-scores of reference BMC (y) / LM (x) correlations obtained from normal people could provide a basis for assessing the anthropometric proportionality between bones and muscles. When a low BMC (or BMD) value in a given individual suggests an osteopenic condition, those z-scores can indicate the nature of such osteopenia. A "normal" z-score of the BMC / LM relationship would indicate that the natural proportionality between bones and muscles is maintained. Such cases may correspond either to a physiological condition (small individuals, otherwise normal) or to a "disuse" osteopenia (a natural mechanostat response to skeletal unloading resulting from a low physical activity). Lower-than-normal z-score values would indicate a failure of the control of bone structure by bone mechanostat as a result of a metabolic disturbance of bone cells. The general hypothesis of this study proposes that osteopenias could be classified this way according to their "disuse" or "metabolic" etiology, respectively.

In fractured individuals, such analysis may determine whether the failure of bone was or was not conditioned by a "metabolic" disturbance. Presumably, this association may vary for fractures in different sites of the skeleton.

Aims and methods. In order to investigate the diagnostic value of that potentially interesting resource, we compared whole-body (WB) and lower-limb (LL) BMC and LM data of 140 pre- and 483 post-MP Hispanic women with fractures produced within the last 2 years in different sites of the skeleton. Their BMC/LM z-scores were calculated with the aid of previously-determined reference curves of WB and LL data from 814 pre- and 1,656 post-MP normal women of comparable ages taken from the same population with the same machine (Lunar DPX, Wisconsin). Women with a history of any illness or treatment that could have affected the skeleton during the last 2 years were excluded.

Results. It was observed that the z-scores corresponding to cases with some particular fracture locations (spine, wrist, arm, leg, and especially hip) were significantly lower than normal ("low-z" fractures, LzFx, n=396; ANOVA, $p<0.001$ in all instances), while those for cases with fractures in any remaining location did not differ from controls ("normal-z" fractures, NzFx, n=227; ANOVA, n.s.), regardless of the women's age or pre- or post-MP condition.

The CMO vs. MM curves for both NzFx and LzFx pre-MP women were similar to the reference curves for both WB and LL (ANCOVA, n.s.). Post-MP women with NzFx behaved similarly but those with LzFx showed non-linear relationships, with dramatically decreasing BMC values toward the lowest LM range (ANCOVA, $p<0.0001$). The standard errors of the estimates (SEE's) of all those curves were average half in LL than in WB determinations.

Interpretation. If our assumptions are correct, 1. the observed spine, wrist, arm, leg, and especially hip fractures seemed to have been more closely associated to a "metabolic" osteopenia (LzFx) than fractures in other locations were; 2. post-MP women had a higher LzFx / NzFx proportion than pre-MP women, so much that the LzFx happened as an almost

exclusive feature of the post-MP women; 3. in post-MP women, the incidence of LzFx increased significantly as LM values decreased (perhaps because of the absence of the enhancement of bone sensitivity to mechanical stimuli induced by sex hormones or related factors); and 4. the determinations performed in the LL would be equally or more reliable than those made in the WB for this diagnostic purpose, hence the required DEXA study could be performed saving a substantial amount of time and cost if the LL region is selected.

Perspective. This novel DEXA diagnosis of the "metabolic" condition of an osteopenia or an osteopenic fracture could be useful in distinguishing cases in which a pharmacological treatment should be indicated ("metabolic" osteopenia) from those in which only a physical therapy may suffice; as well as for monitoring the results of such treatments following biomechanical criteria, at a relatively low cost.

P-11

Comparative Effects of Vitamin K and Vitamin D Supplementation on Prevention of Osteopenia in Calcium-Deficient Young Rats

*J. Iwamoto[1], J. K. Yeh[2], T. Takeda[1]
[1] Department of Sports Medicine, Keio University School of Medicine, Tokyo, Japan,
[2] Metabolism Laboratory, Dept. of Medicine, Winthrop-University Hospital, Mineola, NY, USA
E-mail: jiwamoto@sonata.plala.or.jp

The aim of this study was to clarify the difference in the effects of vitamin K and vitamin D supplementation on the development of osteopenia in young rats under mild calcium deficiency. Sixty female Sprague Dawley rats, 6 weeks of age, were randomized by stratified weight method into six groups with 10 rats in each group: baseline control, 0.5% (normal) calcium diet, 0.1% (low) calcium diet, 0.1% calcium diet + vitamin K (30 mg/100 g), 0.1% calcium diet + vitamin D (25 μg/100 g), and 0.1% calcium diet + K + D. After 10 weeks of feeding, serum calcium, 25-hydroxyvitamin D3 [25 (OH) D3], 1,25-dihydroxyvitamin D3 [1,25 (OH)2 D3], and parathyroid hormone (PTH) levels were measured, and intestinal calcium absorption and renal calcium reabsorption were evaluated. Bone histomorphometric analyses were performed on cortical bone of the tibial shaft and cancellous bone of the proximal tibia. Calcium deficiency induced hypocalcemia, increased serum PTH and 1,25 (OH)2 D3 levels with decreased serum 25 (OH) D3 level, stimulated intestinal calcium absorption and renal calcium reabsorption, and reduced maturation-related cortical bone gain as a result of decreased periosteal bone gain and enlarged marrow cavity, but did not significantly influence maturation-related cancellous bone gain. Vitamin K supplementation in calcium-deficient rats stimulated renal calcium reabsorption, retarded the abnormal elevation of serum PTH level, increased maturation-related cancellous bone gain, and retarded the reduction in maturation-related cortical bone gain. On the other hand, vitamin D supplementation in calcium-deficient rats stimulated intestinal calcium absorption via increased serum 1,25 (OH)2 D3 level with prevention of the abnormal elevation of serum PTH level, prevented hypocalcemia, reduced the maturation-related cancellous bone gain, and prevented the reduction in periosteal bone gain and enhanced enlargement of the marrow cavity with no significant effect on the reduction in maturation-related cortical bone gain. However, no synergistic effect of vitamin K and vitamin D on intestinal calcium absorption, renal calcium reabsorption, and cancellous and cortical bone mass was found. This study shows the differential effects of vitamin K and vitamin D supplementation on the development of osteopenia in young rats under mild calcium deficiency. Vitamin K supplementation stimulates renal calcium reabsorption, increases maturation-related cancellous bone gain, and retards the reduction in maturation-related cortical bone gain, while vitamin D supplementation stimulates intestinal calcium absorption, and prevents the reduction in maturation-related periosteal bone gain by inducing accumulation of calcium from cancellous and endocortical bone.

P-12

A Large-Scale Genome-Wide Scan for QTLS Underlying BMD Variation in an Extended Sample

*Y.Z. Liu[1,2], P. Xiao[1,2], H. Shen[1,2], J.R. Long[1], F.H. Xu[1,2], L.J. Zhao[1,2], Y.J. Liu[1,2], Y.Y. Zhang[1], D.H. Xiong[1,2], S. Araujo[1], V. Dvornyk[1], K.M. Davies[1], T. Conway[1], R.R. Recker[1], H.W. Deng[1,2,3]
[1] Osteoporosis Research Center, Creighton University Medical Center, Omaha, NE, USA, [2]Department of Biomedical Science, Creighton University, Omaha, NE, USA,
[3] College of Life Sciences, HuNan Normal University, Changsha, China
E-mail: yzhliu@creighton.edu

Low bone mineral density (BMD) is a major risk factor for osteoporosis and is under strong genetic control. Previously, we reported a genome-wide linkage scan for BMD in 53 pedigrees with 630 Caucasian subjects (Deng et al., JCEM; 2002). We observed several regions with suggestive linkage. To confirm the previous results and to identify those genomic regions that may have been undetected in the previous study, we performed another whole genome scan in an extended large sample of 79 pedigrees, in which 1,816 individuals were genotyped using 432 microsatellite markers. This current sample contains more than 70,000 relative pairs informative for linkage analyses including 3,846 sibling pairs, which yields dramatic increase in the statistical power and leads to more reliable results for whole genome linkage scan analyses compared to our earlier whole genome linkage study. The number of informative relative pairs contained in this sample represents one of the largest in the human genetics field in whole-genome linkage scan studies for any complex trait. The raw BMD values at spine, hip, and wrist were adjusted for age, sex, weight, and other significant covariates. Two- and multi-point linkage analyses were performed using a variance component method implemented in the computer package SOLAR. Several genomic regions showed suggestive linkage (maximum LOD score, MLS > 1.5) for BMD at spine, hip and wrist, such as 7p15, 11q23, 18q21 and 2q12. Three detected linkage regions (10q26, 11q12 for hip BMD and 11q23 for spine BMD) were replicated with our previous study or other groups' linkage analysis. This study is one of a few genome scans performed in extended samples with larger statistical power.

P-13

A Stereologically Derived Index of Changes in Growth Plate Chondrocyte Morphometry Following Exposure to Irradiation and Pre-treatment With The Radioprotectant Amifostine

*B.S. Margulies, J. Strauss, J.A. Spadaro, T.A. Damron
Upstate Medical University, S.U.N.Y., Syracuse, NY, USA
E-mail: xxxwayfarer@lycos.com

Introduction: Beneficial dose-dependent effects of a free radical scavenger in ameliorating the damaging effects of irradiation on the growth plate have been described.[1,2] Qualitative observations of the temporal changes in chondrocyte profiles observed following irradiation, suggested that chondrocyte size in the reserve and proliferative zones increased transiently after irradiation before gradually returning to a pre-irradiation size. Ideally, an objective evaluation of this hypothesis would be accomplished using unbiased stereology. However, in this instance an experimental design appropriate for a stereologic approach would be prohibitive due to the large number of animals employed in this study and the use of relatively thick 5 μm sections necessary for optimal morphology. Consequently, we developed an morphometric index of chondrocyte size changes that we subsequently validated using stereology.

Methods: In 30 male weanling Sprague Dawley rats, the right proximal tibia and distal femur were exposed to 17.5 Gy irradiation with half of the animals given 100 mg/kg Amifostine (Ethyol) IP 20 minutes prior to exposure.[1,2] Left legs served as internal controls. Animals were then euthanized at 0.5, 1, 2, 3, and 4 weeks following irradiation. Skeletonized tibia were split sagittally and fixed in RHT-glutaraldehyde-paraformaldehyde[3]. Tibia were embedded in MMA and cut at 5 μm for non-stereological analysis or Epon Araldite and cut at 1 μm for stereological analysis. All 30 animals were used for the non-stereological analysis while 4/30 animals were used for the stereological analysis. Volume Fraction (Vf) and Numerical Density (Nv) were determined using stereology. The dissector method was used to determine Numerical Density with the equation: $Nv = (1/(A*T))*(Q/P)$, where A is the area of a test box, T is the distance between sections, Q is the sum of the number counted, and P is the sum of the

number of testing boxes falling within the area of interest. For non-stereological analysis Area Fractions (Af) were calculated and the Number of Cellular Profiles (NCP) were counted. Chondrocyte Indices were calculated (CIndx) by dividing the Volume Fraction by the Numerical Density (CIndx=Vf/Nv) or dividing the Area Fraction by the Number of Cellular Profiles (CIndx=Af/NCP). In both cases the reserve zone was defined as being between the epiphyseal plate and the first proliferative cell. The proliferative zone was defined as being between the first proliferating cell and a point 150 μm distal in the direction of the metaphysis. The hypertrophic zone was defined as extending 150 μm proximally from the chondro-osseous junction in the direction of the epiphysis. Slightly modified definitions had to be employed for the irradiated limb reserve and proliferative zones due to the altered morphology. The reserve zone was defined as the layer of cells immediately below the epiphyseal plate and the proliferative zone was defined by a point 50 μm below the epiphyseal plate; both when no clear first proliferative cell could be identified. ANOVA was used and $p<0.05$ was considered significant.

Table 1		Stereology	Non-Stereology	
	Group	Mean	Mean	% Diff
CIndx	CtXRT	95.01	97.37	2.42%
	CtAMF	80.92	81.82	2.28%
	Xrt	79.10	80.98	2.32%
	Amf	65.22	66.98	2.63%

Results: The mean percent difference in Chondrocyte Index (CIndx) calculated for the two methods was 2.41%. (Table 1) The non-stereological method was then used to calculate CIndx for three animals per treatment group. Control legs treated with amifostine (CtAMF) had a CIndx that was 20% smaller than irradiation group control legs (CtXRT) in the reserve ($p<0.005$) [Figure 1] and proliferative zones ($p<003$). There was no statistical difference found between control legs in the hypertrophic zone ($p>0.09$) [Figure 2]. The CIndx in irradiated leg reserve zone cells treated with and without amifostine were 19% less than corresponding controls at 0.5 weeks ($p<0.01$), increasing to 40% ($p<0.01$) and 12% ($p<0.01$) respectively for the irradiation (XRT) and amifostine (AMF) treatment groups at 1 week. The CIndx for irradiated reserve zone cells was seen to decrease towards controls after 1 week [Figure 1]. The difference between the irradiated limb proliferative zone CIndx and corresponding controls was 50% less in the animals that received amifostine ($p<0.04$). The irradiation treatment group hypertrophic zone CIndx decreased 18% versus controls at 1 week and then increased 20% relative to controls at 3 weeks ($p<0.04$). The amifostine treatment group hypertrophic zone CIndx was 12% less than controls at 0.5 weeks ($p<0.001$) and thereafter was indistinguishable from controls ($p>0.1$). (Figure 2)

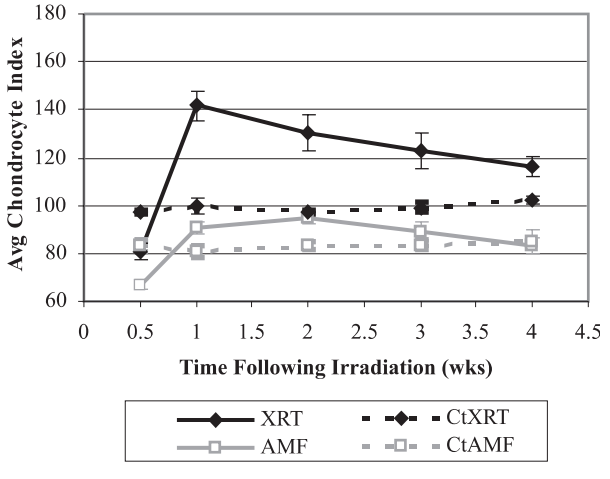

Fig. 1. Reserve Zone CI.

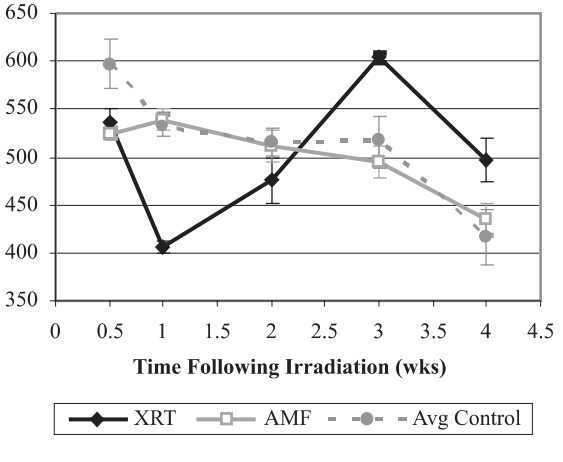

Fig. 2. Hypertrophic Zone CI.

Discussion: The non-stereological index of size changes in growth plate chondrocytes, the Chondrocyte Index, correlates very well with parallel stereological methods. The changes observed with this index also corresponded well with previous qualitative and quantitative observations.[1,2] Additional novel observations regarding the amifostine effects were made using this method. First, amifostine, independent of its radioprotectant effects, reduced reserve and proliferative zone cell size; whereas it did not affect hypertrophic zone cells. Second, radiation had an effect, independent of amifostine, that causes reserve zone cells to be smaller than controls at 0.5 weeks. Most importantly, amifostine had a clear normalizing effect with respect to preserving growth plate chondrocyte morphology following irradiation therapy.

Acknowledgments

CN Farnum, Cornell for guidance. This work has been funded in part by grants from The Children's Miracle Network and NIH NCI RO1:CA83892.

References

1. Damron TA, Margulies BS, Strauss JA, O'Hara K, Spadaro JA, Farnum CE. Sequential histomorphometric analysis of the growth plate following irradiation with and without radioprotection. J Bone Joint Surg Am 2003; 85-A:1302-1313.
2. Margulies B, Morgan H, Allen M, Strauss J, Spadaro J, Damron T. Transiently increased bone density after irradiation and the radioprotectant drug amifostine in a rat model. Am J Clin Oncol 2003; 26:E106-114.
3. Hunziker EB, Herrmann W, Schenk RK. Improved cartilage fixation by ruthenium hexammine trichloride (RHT). A prerequisite for morphometry in growth cartilage. J Ultrastruct Res 1982; 81:1-12.

P-14

Effects of Vitamin D and Estrogen Receptor Gene Polymorphisms on the Changes in Lumbar Bone Mineral Density With Multiple Pregnancies in Japanese Women

*H. Matsushita, T. Kurabayashi, K. Tanaka
Department of Ob/Gyn, Niigata University School of Medicine, Niigata, Japan
E-mail: hiroshi.matsushita@utah.edu

Background: Multiple pregnancies are not generally considered a risk for decreasing peak bone mass of women, even when women were grand multiparous. However, it is not clearly understood whether peak bone mass was similarly maintained in all women, in all circumstances. It is likely that variation in the results arose due to the individual's age, or aspects of their social, environmental, hormonal or nutritional background. Recently, the importance of genetic interactions on bone metabolism has been noted, and polymorphisms in the vitamin D receptor (VDR), and the estrogen receptor (ER) genes have been reported to have associations with bone mineral

density (BMD).

Methods: The BMDs of the lumbar spine (L2-L4) of 133 healthy women who had undergone two successive pregnancies were repeatedly measured within 7 days after each delivery. Seventy-three non-pregnant and healthy women were included as controls. The restriction fragment length polymorphisms were analyzed using restriction endonucleases TaqI, ApaI, and FokI for the VDR gene, and PvuII and XbaI for the ER gene.

Results: The mean percent change in BMD (ΔBMD%) of all the 133 women was significantly higher than that of the control (1.4 ± 4.0% vs. 0.1 ± 3.6%; P = .025, unpaired t-test). ΔBMD% of the women with the XX/Xx genotype was significantly lower than that of the women with the xx genotype (0.2 ± 3.3 vs. 2.0 ± 4.2%; P = .030, ANCOVA). Multiple regression analyses to evaluate the contribution of the XbaI polymorphism of the ER gene on ΔBMD% showed that the percentage decrease in BMD was greater for women lacking the XbaI restriction site (R2= .188, P < .0001).

Conclusions: The longitudinal changes in BMD with multiple pregnancies were significantly influenced by the XbaI polymorphism of the ER gene. In addition, the percentage change in BMD was negatively correlated with the absence of the XbaI restriction site.

P-15

RHBMP-7 Induced Posterior Spinal Fusion in Female Rats is Dependent on Estrogen Status

*P. Moazzaz, M.C. Gupta, S. Maitra, M. Gilotra, R.B. Martin, A.H. Reddi, J Chen
University of California, Davis School of Medicine, Sacramento, CA, USA
E-mail: pmoazzaz@ucdavis.edu

Introduction: Rat spinal fusion has been established as a consistent, efficient model for lateral intertransverse process lumbar fusions. Previous experiments have confirmed the efficacy of pellets containing Insoluble Collagen Bone Matrix (ICBM) and rhBMP-7 in producing a successful lateral intertransverse process single level lumbar fusion in a rat model. Studying these implications in an osteoporosis model is of clinical value as many patients undergoing spinal fusion surgery exhibit osteoporosis. This group of patients is expected to rise in the future. The purpose of our study was to examine fusion rates in intact and ovariectomized (OVX) estrogen-deficient female rats using rhBMP-7. Methods: Fifteen OVX and fifteen sham operated Sprague Dawley female rats were randomly assigned to groups receiving 25mg ICBM, 25mg ICBM+10mcg rhBMP-7, and 25mg ICBM+30mcg rhBMP-7. Spinal fusion was evaluated by manual motion testing at each lumbar segment, and radiographic evaluation using the Lenke grading system.

Results: OVX and intact rats receiving 25mg ICBM alone did not demonstrate any spinal fusion. With 25mg ICBM+10mcg rhBMP-7, there was not a significant difference in fusion rates between intact and OVX rats (P=0.63). In the 25mg ICBM+30mcg rhBMP-7 group, 6/6 intact rats were fused, while 6/6 OVX rats displayed motion across the segment. Radiographic analysis with Lenke grading concurred with these findings, thus demonstrating significantly lower fusion rates in OVX rats as compared to intact rats (P=0.013).

Conclusions: Spinal fusion is negatively affected by estrogen deficiency. RhBMP-7 was unable to overcome to the detrimental effects of estrogen deficiency on spinal fusion.

P-16

Bone Lesions in the Hemochromatosis of Salers Cattle

R.W. Norrdin[1], K.H. Hoopes[1], D. O'Toole[2]
[1] Colorado State University, Fort Collins, CO,
[2] University of Wyoming, Laramie, WY, USA
E-mail: rnorrdin@lamar.colostate.edu

Hemochromatosis in Salers cattle is a familial wasting disease characterized by accumulation of iron and death due to liver failure in young adults (O'Toole et al., Vet Pathol 2001; 38:372). Soft bones and incisor loss have been reported but skeletal lesions have not previously been examined in detail.

An affected heifer from a colony at Wyoming State Veterinary Laboratory was monitored from birth until euthanasia at 18 months. An unaffected, age-matched animal was used for comparison. The heifer fell two weeks before euthanasia, developed non-weight-bearing lameness of the right forelimb, then became recumbent and lost weight rapidly. Both animals received fluorescent bone markers 5 and 12 days before euthanasia.

At necropsy, the heifer had fractures of the right humerus, left femur, and two ribs. The cortex was thicker in long bones of the affected heifer when compared to the control. Distinctive circumferential light-dark laminations in the outer third of the cortex were visible along the shafts of long bones and the mandible. These were seen radiographically as layers of decreased density. Bone analysis revealed iron levels in the affected calf that were 30 to 50 times greater than the control and decreased % ash in the outer cortex. Histologically there were irregular layers of osteopenic outer circumferential lamellae and decreased mineralization where excess iron was found in the matrix. The fluorescent marker indicated irregular mineralization in the outer cortical layers of the affected heifer. Endochondral bone formation beneath the growth plate in the affected heifer was markedly decreased as compared to the control.

Results indicate that in hemochromatosis, there are increased iron levels in the bone matrix that are associated with dysplastic periosteal bone formation. There is periodic inhibition of osteoblastic bone formation and mineralization in the outer cortex. Cortical defects led to weakening and pathologic fractures.

P-17

Assessment of Mouse Bone Metastasis by *In Vivo* Micro-CT

P.L. Salmon[1], R. Nuydens[2], H. Vermeirsch[2], E. Buelens[1], A. Sasov[1]
[1] Skyscan N.V., Aartselaar, Belgium,
[2] Johnson & Johnson Pharmaceutical Research & Development, Beerse, Belgium
E-mail: phil.salmon@skyscan.be

Bone tissue is rich in a variety of growth factors, and provides a fertile soil for cancer cells to develop into metastases due to the release of these growth factors during osteoclastic bone resorption[1]. A number of mouse models have been developed in the past few years for both metastasis and myeloma. In this study *in vivo* micro-CT is evaluated for its ability to provide information *in vivo* on the extent of bone metastasis damage which can be correlated with clinical signs of cancer bone pain. Cultured tumor cells were injected directly into the distal femur of mice. The injected doses were 100,000 cells (4 mice), 500,000 cells (2 mice) and none (control, 2 mice). Pain was assessed by evaluating the development of hyperalgesia indicated by limb-lifting, assessing knee swelling and by nociceptive tests. Mice were killed prior to micro-CT imaging (Skyscan 1076), and the hindlimbs were amputated but the bones were not dissected out, replicating *in vivo* micro-CT scanning conditions. Primary micro-CT assessment of bone tumour extent was by visual inspection of 3-D rendered models of the scanned bones. This allowed sensitive and early detection of porosity and structure loss due to tumor. A striking feature observed was extracortical quasitrabecular calcification in some tumor-affected bones. Morphometric parameters of control and tumor affected femurs were assessed as a longitudinal profile of cross-section measurements moving from the epiphysis through the growth plate toward the midshaft. Sectional bone volume and Euler number gave sensitive indication of the degree of tumor damage. Thickness distribution measured in 3-D over the whole distal femur showed the effects of structure loss from tumor osteolysis as a shift to lower structure thickness. Alterations in the pain measurements correlated generally with the degree of bone destruction as quantified by morphometric parameters.

Reference

1. Yoneda T, Michigami T, Yi B, Williams PJ, Niewolna M, Hiraga T. Actions of bisphosphonate on bone metastasis in animal models of breast carcinoma. Cancer 2000; 88(Suppl. 12):2979-2988.

P-18

Performance of *In Vivo* Micro-CT Analysis of Rodent Trabecular Bone Architecture

P.L. Salmon[1], E. Buelens[1], A. Sasov[1], E. Waarsing[2]
[1] Skyscan N.V., Aartselaar, Belgium,
[2] Department of Orthopaedics, Erasmus Medical Centre, Rotterdam, The Netherlands
E-mail: phil.salmon@skyscan.be

Micro-CT analysis of trabecular bone, both *ex vivo* and more recently *in vivo* for rodent preclinical models, has made possible more powerful analysis of trabecular architecture in the last decade. *In vivo* micro-CT analysis of rodent trabecular bone allows the possibility of sequential analysis of a bone site in a single animal. However there are several factors limiting the quality of micro-CT images of trabecular bone obtainable *in vivo*. X-ray image contrast is reduced by the presence of surrounding soft tissue causing additional attenuation. The source and detector geometry imposed by an immobile subject limits pixel sizes attainable compared to *ex vivo* micro-CT systems. Repeated bone morphometric parameters measured by micro-CT are presented for a standard sample (a mouse vertebra) using the Skyscan 1076 *in vivo* and 1072 *in vitro* scanners. Calibration measurements of aluminium phantoms are also presented. Repeatability of measured parameters is assessed, as is the sensitivity of morphometric parameters to pixel size. Histomorphometric parameters show differing sensitivity to varying image resolution and contrast. Structure model index and Euler connectivity are acutely sensitive to image resolution. We demonstrate that despite the above mentioned constraints on *in vivo* microCT image resolution, useful and representative architectural parameters of mouse trabecular bone can be obtained by micro-CT *in vivo*. Ideally pixel size should be less than 10 micron and the 10 percent MTF resolution below 15 micron for mouse trabecular analysis. The sequential imaging of a bone site in a rodent, allows the technique of image registration to be applied (with appropriate calibration of registration error), giving new histomorphometric possibilities for measurement and imaging of bone formation and resorption during a study period. Unlike conventional dynamic histomorphometry, this technique allows resorption as well as formation to be visualised and quantified.

P-19

Two-Dimensional and Three-Dimensional Culture of Human Bone Marrow Stromal Cells With Different Scaffolds

*HX. Sang, P.P. Lin, C.A. Savary, K.L. Weber, V.O. Lewis, F. Jin, A.W. Yasko
University of Texas M.D. Anderson Cancer Center, Houston TX, USA
E-mail: hx_sang@yahoo.com

Bone marrow stromal cells (BMSC) are proven to be an ideal source of osteoblastic progenitors. We evaluated the optimal culture method for human BMSC *in vitro* in 2-dimensional (2-D) culture plate or in 3-dimensional (3-D) culture system with different scaffolds. Fresh human bone marrow samples were aspirated and mononucleated cells were separated, cultured in α-MEM supplemented with 15% FCS with or without differentiation reagents consisting of ascorbic acid, β glycerophosphate and dexamethasone (Dex). BMSC passages 2 – 6 were used for co-culture with scaffolds of human freeze-dried cancellous granules (MTF), β-TCP and poly (propylene fumarate, PPF) respectively, either in the static culture plate or in a rotating vessel bioreactor. The BMSC were characterized by MTT and ^{3}H thymidine proliferation assays, ALP and von Kossa staining, colony forming units assay, RT-PCR assay of osteocalcin (OC) and Parathyroid hormone-related protein (PTHr-P) expression and FACS analysis of the cell surface markers. Histological section and scanning electron microscope exam were used to evaluate the interaction between the BMSC and scaffolds. As a result, culture conditions were optimized for expanding and differentiating BMSC from the fresh human BM towards the osteoblastic cells. The media and the batch of the FCS were critical for the BMSC proliferation and colonies formation. The ascorbic acid, β glycerophosphate and Dex were necessary for the BMSC to differentiate towards osteoblast, which were evidenced by high ALP and OC expression. However, high concentration of DEX ($>10^{-7}$ M) inhibited the proliferation of BMSC. The MTF cancellous granules were proven more suitable for BMSC attachment and proliferation compare to other scaffolds. In 3-D culture, the BMSC were mainly surrounding the scaffold network and forming a periphery liner aggregation. After 4 weeks, lots of bone matrix secreted and the "woven bone " like structures formed surrounding as well as inside the porous of the cancellous scaffolds. As a conclusion, MTF scaffolds best supported the BMSC proliferation and differentiation under critical culture conditions in static or bioreactor 3-D culture system. The 3-D culture system of BMSC with different scaffolds may be used to evaluate the biocompatibility of the new bone substrates and to mimic the tissue engineering bone growth.

P-20

Effect of Bisphosphonate on Bone Fracture Healing in Cynomolgus Monkeys

A. Seki[1], K. Nonaka[2], T. Ishii[3]
[1] HAMRI Co. Ltd., Tokyo, Japan,
[2] ELK Corporation, Tokyo, Japan,
[3] Maruto Instrument Co., Ltd., Tokyo, Japan
E-mail: a_seki@hamri.co.jp

Objective: The Cynomolgus monkey exhibits a similar bone remodeling and bone metabolism manner to humans. In this study, the effect of an antiresorptive drug on fracture healing was evaluated using Cynomolgus monkeys.

Animals and method: Four female cynomolgus monkeys 9 years of age raised in our facility were used. The bone fracture model was prepared by surgically cutting the diaphysis of left femur under anesthetic and sterile conditions. The surface of the periosteum was applied with a mini-plate fixed with screws at 3 sites each on the proximal and distal side of the wounded portion. Two of them were administered with physiological saline and others were administered with alendronate at 0.05 (ALN 0.05) and 0.25 mg/kg (ALN 0.25), respectively. Dosing was carried out subcutaneously at dorsal region once every 2 weeks for 24 weeks. Healing condition was observed by taking X-ray photography of the fracture site once every 2 weeks from 1 week after the surgery. After completion of the dosing period, femurs were collected and preserved frozen. Those samples were scanned with 0.77mm of slice thickness and 0.3mm of voxel size by peripheral quantitative computed tomography (XCT Research SA+, Stratec, Germany). A total of 9 CT slices around the wounded portion of fracture site and 3 slices of the mid-diaphysis of non-fracture site were obtained. Then three-point bending test was performed using a bone strength analyzer (MZ-500S, Maruto Co., Ltd).

Results: In ALN animals a callus had been formed after 2 weeks and was progressively calcified and enlarged until 6 weeks. The callus formation was quicker in ALN-treated animals than in physiological saline-treated animals. Although no marked difference was noted between the ALN-treated animal at 0.05mg/kg and one at 0.25mg/kg, a fracture line was more obviously noted in the latter than in the former after dosing for 24 weeks.

Cortical bone density was lowest in the fracture site and became gradually higher moving away from the fracture site. Cortical bone density of the animals given ALN was higher than one of control animals at any site. Cortical bone thickness at the fracture site was thicker than at the other sites in the animal of ALN 0.25, and was not different at all sites in the animal of ALN 0.05. In the control animals, cortical thickness at the fracture site was thinner comparing to one of the other site.

Mechanical test for non-fractured femurs showed that ALN-treated animals had higher breaking deformation and breaking energy than in control animals. The breaking deformation for fractured femur of ALN 0.05mg was equal to that of control animals, and both of breaking force and energy of ALN 0.05 were higher than those of controls. In ALN 0.25 fractured femur, breaking energy was higher, and both breaking force and deformation was lower than those of the controls.

Discussion and conclusion:

(1) Absorption of callus was delayed by ALN administration.

Fracture line was still obvious after 24 weeks of ALN administration at 0.25mg/kg, suggesting that fracture healing was much delayed at the dosage level.

P-21

Persistent Osteopenia in a Thermal Injury Mouse Model

*J.E. Shea, B.M. Bowman, S.C. Miller
Division of Radiobiology, University of Utah School of Medicine, Salt Lake City, UT, USA
E-mail: j.shea@m.cc.utah.edu

Introduction: Severe burns are associated with altered skeletal metabolism including losses of bone mass, retardation of growth velocity, and reduced bone formation with a consequent increased risk of fractures and potentially life-long osteoporosis[1]. The thermal injury mouse model has been utilized to investigate skeletal alterations at 10 days post-burn[2,3]. However, the longer-term skeletal alterations have not previously been examined. Therefore, the goal of the current study was to investigate the effect of thermal injury on skeletal metabolism one month post-burn in a mouse model.

Materials and Methods: Young adult male Balb/c mice were divided into baseline control, sham burn, and burn groups (n=10). A full thickness scald burn was applied to the back following a previously published protocol[2,3]. The fluorochrome bone marker calcein (15 mg/kg) was given 6 and 1 days prior to necropsy by subcutaneous injection. Whole body BMC and BMD were determined 2 days prior to thermal injury and immediately prior to necropsy with peripheral dual energy X-ray absorptiometry (pDXA). After necropsy, the proximal tibias were embedded in methylmethacrylate and utilized for static and dynamic histomorphometric analysis.

Results: There was a greater decrease in whole body and hind limb BMD and hind limb BMC in the burn group compared with the sham group ($p < 0.05$). The endochondral growth rate at the tibial epiphysial plate was lower in the burn (12.75 ± 0.6; mean ± SE) than the sham (14.52 ± 0.61) and the baseline (17.25 ± 0.94)($p<0.05$). There were no differences in the % double-labeled surface, mineralizing surface (MS), or mineral apposition rate (MAR) between the three groups in the cancellous bone of the proximal tibia. However, the percent bone was lower in the burn (1.2 ± 0.1) than in the sham (7.3 ± 0.5) and the baseline group (8.0 ± 1.1)($p<0.05$).

Discussion: The skin at the burn site had completely healed at the end of one month, which also coincided with a restoration in MAR and MS. Despite the MAR and MS returning to baseline levels, there was still a suppression of endochondral growth and a persistent osteopenia. The persistent osteopenia is explained by the fact that entire areas of cancellous bone are completely lost and there is no physiological process whereby these can grow back. In conclusion, by one month post-burn the wounded skin has healed and MAR are at baseline levels, but the animals remained osteopenic with stunted endochondral growth.

References

1. Klein GL, Herndon DN, Langman CB, Rutan TC, Young WE, Pembleton G, Nusynowitz M, Barnett, JL, Broemeling LD, Sailer DE, McCauley RL. Long-term reduction in bone mass after severe burn injury in children. J Pediatr 1995; 126:252-256.
2. Edelman LS, Phil M, Shao W, Miller SC, Bowman BM, Morris SE, Shelby J. Effects of burn injury on bone and growth in a mouse model: the 1997 Lindberg Award. J Burn Care Rehabil 1997; 18:483-489.
3. Miller SC, Bowman BM, Siska CC, Shelby J. Effect of thermal injury on skeletal metabolism in two strains of mice. Calcif Tissue Int 2002; 71:429-436.

P-22

Bone Tissue Engineering: Optimization For Load Bearing Applications

*M. Liebschner
Rice University, Department of Bioengineering, Houston, TX, USA
E-mail: Liebschner@rice.edu

Introduction: As our populations age worldwide, we will witness a dramatic increase in the number of fractures associated with osteoporosis. Therefore, there is a dire need for an effective preventive measure that can decrease the incidence of these fractures. A potential intervention recently proposed, percutaneous vertebroplasty, involves fortification of osteoporotic vertebral bodies with an injected bone cement, poly(methyl methacrylate) (PMMA). However, the Food and Drug Administration recently issued a warning on the numerous side effects of bone cement. Alternative bone substitutes with desired mechanical properties need to be found. The goal of this study was to investigate ideal biomechanical properties of alternative biomaterials and their usage in prophylactic, vertebroplasty. Our specific research questions were: 1) how do mechanical properties of the injected material affect the vertebral body biomechanics? and 2) can tissue engineering principles be used to design an ideal material for prophylactic vertebroplasty?

Method: An anatomically detailed and specimen specific finite element model of a human vertebral body was generated from quantitative computed tomography scans and calibrated to experimental results. Bipedicular vertebroplasty using 20% volume fill of bone cement with varying material properties was simulated. The stiffness and fracture load of the virtually treated vertebra under uniaxial compression were predicted using ABAQUS. The effect of design parameters on the mechanical properties of the injectable material was investigated utilizing a combination of CAD and rapid prototyping. Optimization of the material was accomplished by comparison of the geometric shapes to standardized values for normal trabecular bone. A novel injectable bone cement was created using a Calcium Phosphate slurry with solid phase polypropylene fumarate (PPF) particulates of engineered architecture.

Results and conclusion: Varying cement strength, while keeping elastic modulus constant did not affect the structural behavior of the augmented vertebral body since failure of the vertebral body occurred within the weaker trabecular bone. Conversely, increasing cement modulus, while maintaining strength only resulted in increases in vertebral stiffness. The sensitivity of vertebral stiffness with cement modulus indicated that softer and weaker bone cement materials could result in the same strengthening effect, but with reduced stiffness augmentation, minimizing the 'stress-riser' effect. By using a composite material consisting of a liquid and solid phase, an ordered pore structure can be generated. The cured material may promote bone growth and could ultimately improve the biomechanical quality of the regenerated bone tissue. The distinct architectures created in the scaffold will offer variability in mechanical strength and porosity. Such information may lead to refinement of the surgery, improved patient selection, and ultimately, more confidence and successful use of this procedure.

P-23

A Large-Scale Whole Genome Scan For QTLs Influencing Bone Size Variation in an Extended Sample: Suggestive Linkage on 14Q32, 11Q12 and 17Q22

*H. Shen[1,2], D.H. Xiong[1,2], F.H. Xu[1,2], J.R. Long[1], P. Xiao[1,2], L.J. Zhao[1,2], Y.Y. Zhang[1], Q. Zhou[1], Y.J. Liu[1], Y.Z. Liu[1,2], V. Dvornyk[1], S. Araujo[1], K.M. Davies[1], T. Conway[1], R.R. Recker[1], H.W. Deng[1,2,3]
[1] Osteoporosis Research Center,
[2] Department of Biomedical Sciences, Creighton University Medical Center, Omaha, NE, USA,
[3] College of Life Sciences, HuNan Normal University, ChangSha, HuNan, P. R. China
E-mail: huishen@creighton.edu

Bone size, as an important risk factor for osteoporotic fractures, is highly heritable. Previously, we reported a genome wide linkage scan for bone area phenotypes (measured by DXA) in 53 pedigrees with 630 Caucasian subjects that contained more than 10,000 informative relative pairs including 1,249 sibling pairs (Deng et al., AJMG, 2002). A significant linkage was found in genomic region 17q22 for the wrist bone size. We also observed several regions with suggestive linkage. To confirm the previous results and to identify those genomic regions that may have been undetected in the previous study, we performed another whole genome scan in an extended large sample of 79 pedigrees, in which 1,816 individuals were genotyped using 432 microsatellite markers. This current sample contains more than 70,000 relative pairs informative for linkage analyses including 3,846 sibling pairs,

which yields dramatic increases in the statistical power and leads to more reliable results for whole genome linkage scan analyses compared to our earlier whole genome linkage study. The number of informative relative pairs contained in this sample represents one of the largest in the human genetics field in whole genome linkage scan studies for any complex trait. We detected suggestive linkage for several genomic regions (e.g., 14q32, Maximum LOD score = 2.61) that have not been identified in our earlier whole genome scan. In addition, suggestive evidence for replication with our previous results has been found on chromosome 17q22. These findings demonstrate the importance of large sample size and statistical power in the whole genome scans to search for genes underlying the complex traits such as bone size.

P-24

Fracture Repair in COX-2 Deficient Mice is Not Accelerated by Low Intensity Pulsed Ultrasound

Y. Mikuni-Takagaki[1], H. Sekiya[2], K. Naruse*[3], M. Itoman*[3], K. Seto*[2]
[1] Oral Biochemistry, Kanagawa Dental College, Yokosuka, Japan,
[2] First Dept. of Oral and Maxillofacial Surgery, Tsurumi University School of Dental Medicine, Yokohama, Japan,
[3] Orthopedic Surgery, Kitasato University School of Medicine, Sagamihara, Japan
E-mail: yukomtak@kdcnet.ac.jp

Cyclooxygenase-2 (COX-2) has been shown to play an essential role in bone formation during fracture repair. We have reported that low-intensity pulsed ultrasound (US), which mechanically accelerates fracture healing 40% by time, targets osteoblasts but not osteocytes, and that the anabolic response of osteoblasts was obliterated by blocking COX-2 with NS398 (JBMR; 2003). Therefore, in order to substantiate a fundamental role of COX-2 in the mechanotransduction pathways, acceleration of fracture repair by US was studied in 52±2-week COX-2-/- mice (B6; 129S7-Ptgs2tm1 Jed, Jackson Laboratories), which were subjected to a mid-diaphyseal femoral fracture with intramedullary fixation. Half of the animals in each group were exposed to the anabolic ultrasound from the fourth day of surgery for 20 min a day with a SAFHS (Smith & Nephew Inc.) equipped with probes 13-mm across (Teijin Limited). Conditions were identical to those used for patients and bone cell cultures of rodents and men. Bone formation in these relatively old mice during skeletal repair was monitored by contact X-ray, microCT, histochemical analysis, and real-time PCR. Radiographs and histologic sections of COX-2-/- and wild-type mice after 20-day post-fracture point, all wild-type femora exposed to US attained bony union while untreated COX-2-/- femora neither produced union nor mineralized callus. While some untreated wild-type femora reached union, COX-2-/- callus in exposed femur were poorly mineralized. We found that the amplified late upregulation of mRNAs such as IGF-I, which we reported in US-exposed cells, was lost in COX-2-/- osteoblasts. Taken together, these results suggest that COX-2 not only plays an important role in fracture repair, but also functions as an essential mediator of mechanotransduction leading to bone formation.

P-25

Walking is a Pre-requisite for Parathyroid Hormone Function as an Effective Anabolic Agent in Rat Tibial Cortex

Y. Mikuni-Takagaki[1], K. Aoki[2], M. Takahashi*[2], M. Itoman*[3], K. Ohya[2]
[1] Kanagawa Dental College, Yokosuka, Japan,
[2] Tokyo Medical and Dental University, Graduate School, Tokyo, Japan,
[3] Kitasato University School of Medicine, Sagamihara, Japan
E-mail: yukomtak@kdcnet.ac.jp

Daily subcutaneous injections of low doses of parathyroid hormone (PTH) reduce incidence of osteoporosis-related fractures. The purpose of this study was to characterize synergy between PTH and walking *in vivo*. While the ovariectomized rats provide an excellent animal model for postmenopausal osteoporosis, no such models were available for generalized disuse osteopenia. In our experiment, thirty-week-old female Wistar rats were either restricted by housing them in cages of limited space, W95: L150-130 from top to bottom: H110-55 (at the lowest part of the wirework where pellets were kept), or allowed walking in institutional standard cages. Rats were injected subcutaneously with 10 μg/kg human PTH (1-34) (Asahi Chemical Co.) or saline three times a week for 6 weeks. Calcein was injected twice for measuring mineral apposition rate (MAR). After measuring tibial BMD by pQCT, histomorphometric analysis was carried out by confocal microscopy. Proximal cortical BMD at 6 weeks showed a significant difference between the restricted/saline and walking/PTH with synergistic effect between PTH and walking. No such synergy was present in soleus or gastrocnemius muscle weights and no significant difference, among non-weight-bearing clavicles of all four groups. Further analysis of cortical bone formation rate (BFR) by dividing the transverse plane into five areas showed that bone expands in different manners with walking/saline, walking/PTH, and restricted/PTH conditions, as compared to restricted/saline. Subtracted by the BFR of restricted/saline rat bone, ΔBFR by walking alone (in walking/saline) demonstrated bone drift to the anterior-lateral direction along the neutral axis, while walking/PTH does so to the posterior-medial direction. The supra-additive increase by walking and PTH occurs mainly in the endocortical bone by the increased MAR. In contrast, PTH alone generally expands periosteal bone even in restricted rats, mainly by increasing MS/BS. The expansion is accompanied by periosteocytic calcein labels, suggesting that osteocytic activity is involved. RT-PCR experiments using pulverized cortical bone showed a significant difference in messages such as COX-2 and IGF-I, between walking/PTH and others. From these results, we conclude that PTH and walking act synergistically at a tissue level in tibial cortical bone.

P-26

Muscle Pump-Assisted Flow Through Tissue Engineered Bone Scaffolds: A Capillary Filtration-Based Hypothesis

H. Winet[1,2], C. Caulkins[2], J.Y. Bao[1]
[1] Bone Chamber Laboratory, Orthopaedic Hospital/UCLA, USA,
[2] Biomedical Engineering Department, UCLA, Los Angeles, CA, USA
E-mail: hwinet@laoh.ucla.edu

Introduction: Tissue engineered scaffolds require vascularization to 1) enhance nutrient exchange and 2) provide cells needed to build new tissue. Cell-seeded scaffolds-bioreactors-require rapid penetration of vessels or enhanced fluid percolation to keep their contents alive until normal nutrient exchange can be established. Bone interstitial fluid flow (BIFF) depends on a pumping system which drives percolation through its own matrix. Recent interest in the pumping mechanism has resulted in BIFF models which link the pumps to bending of bone by muscle contraction and compression-tension cycles from weight-bearing during locomotion. We here propose that capillary filtration, the source of the percolating fluid, is sufficiently enhanced by soliton pressure waves in blood driven by the skeletal muscle pump during exercise to provide a significant hydraulic pressure component to bone fluid percolating through bone and any implanted non-vascularized scaffold it contains.

Methods: In support of this hypothesis, we propose experiments employing optical bone chamber implants (OBCI) with intravital microscopy (IVM) as a method for observing capillary filtration-assisted percolation and resultant scaffold perfusion. As a first step in this approach we have employed OBCI IVM to test the underlying hypothesis that muscle pump-driven capillary filtration in bone is convective. OBCIs were implanted in adult NZW female rabbits. Chamber construction and implantation were as usual[1]. At the third week post-op chamber ends were exposed and weekly IVM commenced. Transcutaneous electrical stimulation was administered with a ToneATronicβ TENS at 85V, 80mA and 2Hz. The stimulator was applied externally over the gastrocnemius muscle. A fluorescence digital image was obtained before 30 minutes after application of TENS. FITC-D70 was injected in an aural vein before and RITC-D70 after stimulation. Blood samples were obtained from a vein in the ear opposite that being injected with the fluorescent dye. Concentration of dye was determined with a SPEX Fluoromax-3 spectrofluorometer for both serum and whole blood (to detect differences which would make fluorescence in vessels an inaccurate indicator of concentration due to RBC color contamination). For analysis 4 vessels were chosen and the average

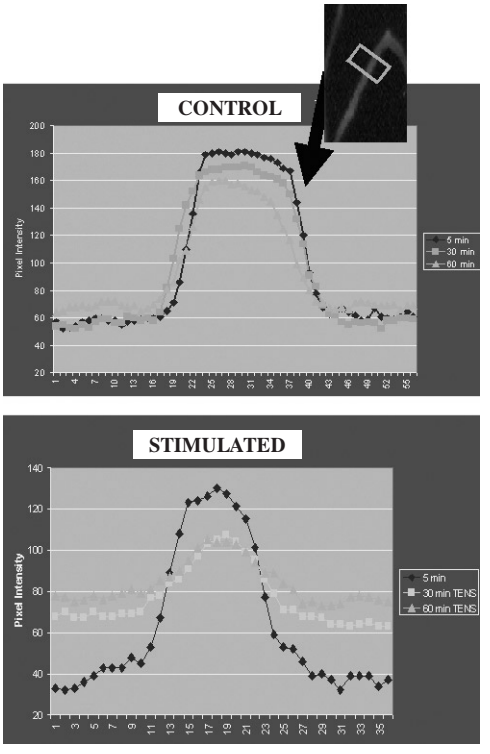

Figure 1. Pixel intensity profiles showing distribution of FITC-D70 as a function of distance from the vessel shown in the uppermost panel. Capillary filtration over 60 minutes of unstimulated (left graph) and muscle pump/TENS-stimulated (right graph) bloodflow. Rate of profile spread is directly proportional to capillary filtration rate in an unbounded fluid. In the bone chamber, however, the fluid is bounded by its windows, so the relationship is much more complex and cannot be evaluated using the simple form of the Nakamura-Wayland equation.

dye concentration profiles extending from within the vessel through adjacent extravascular space were obtained before and after 30 minutes of stimulation.

Results: Results are shown in Figure 1. Values were not calibrated and should be considered relative only. Extravasated dye levels in TENS rabbits were markedly higher than those in controls. Analysis of profiles using an erfc-based diffusion-convection discrimi-nation model[2] showed that extravasation was convective.

References

1. Winet H. A horizontal intravital microscope bone chamber system for observing microcirculation. Microvasc Res 1989;105-114.
2. Nakamura Y, Wayland H. Macromolecular transport in the cat mesentery. Microvasc Res 1975; 9:1-21.

P-27

Bone-Targeted Drug Delivery Systems: A Preliminary Study

*D. Wang[1], S.C. Miller[2], M. Sima[1], P. Kopecková[1], J. Kopecek[1,3]
[1] Department of Pharmaceutics & Pharmaceutical Chemistry/CCCD,
[2] Department of Radiobiology,
[3] Department of Bioengineering, University of Utah, Salt Lake City, UT, USA
E-mail: jindrich.kopecek@m.cc.utah.edu

Introduction: With recent developments in bone biology, many therapeutic targets have been identified for the treatment of bone diseases. Cathepsin K inhibitors, avb3 integrin antagonist, H+-adenosine triphosphatase (H+-ATPase) inhibitors, and carbonic anhydrase II (CA2) have been used as anti-resorptive agents, whereas parathyroid hormone (PTH), prostaglandins E series (PGEs), statin, and bone morphogenetic proteins act as bone anabolic agents[1]. However, the poor tissue specificity of these therapeutic agents has hampered their potential clinical application.

In this study, we have designed and synthesized bone-targeting delivery systems based on N-(2-hydroxypropyl) methacrylamide (HPMA) co-polymers. These are expected to improve the efficacy of many bone-related therapeutic agents.

Experimental methods: HPMA co-polymer conjugates with the general structure shown below were synthesized via free radical co-polymerization and polymer-analogous reaction.

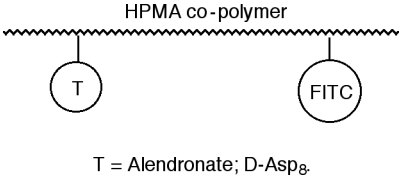

Figure 1. General structure of bone-targeting delivery system based on HPMA copolymers. Fluorescein isocyanate (FITC) was used as a model drug.

Results and discussion: There are many advantages in a bone-targeted drug delivery system to be realized for the treatment of bone diseases. Bone-targeting moieties, such as bisphosphonates[2], tetracycline[3], glutamic acid oligopeptide and aspartic acid oligopeptide[4], have been conjugated to therapeutic agents to render them osteotropic. In the present study, we have conjugated alendronate and D-aspartic acid octapeptide to HPMA co-polymer, which contains FITC (fluorescein isocyanate) as a model drug to facilitate the analysis of *in vitro* and *in vivo* binding studies. Acid or enzyme cleavable bonds may be used to attach therapeutic agents to the polymer backbone and to limit the release of drug to the target sites.

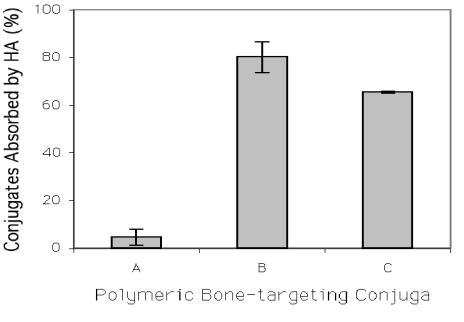

Figure 2. *In vitro* binding efficiency to hydroxyapatite of bone-targeted HPMA co-polymer conjugates. A. P-FITC; B. P-(D-Asp8)-FITC; C. P-alendronate-FITC.

In the *in vitro* study, both bone-targeted conjugates (P-alendronate-FITC and P-D-Asp8-FITC) strongly bound to hydroxyapatite, while the control polymer P-FITC (HPMA without a targeting moiety) only showed non-specific binding (Figure 2).

Conjugate targetability to bone was also evaluated *in vivo*. For this, all three conjugates were i.v. injected into balb/c mice. Saline was injected into another group of mice as a control. After 24 h, the long bones were collected and prepared for histomorphometric analyses. Both bone-targeting conjugates, P-alendronate-FITC and P-D-Asp8-FITC, showed very strong fluorescence staining in bone, while the two control groups (saline and P-FITC injection) revealed no fluorescence in bone (Figure 3). Furthermore, the bone-targeted HPMA copolymer conjugates appeared to accumulate at the bone growth sites where the blood supply is abundant.

Conclusion: Preliminary data presented here demonstrated a strong

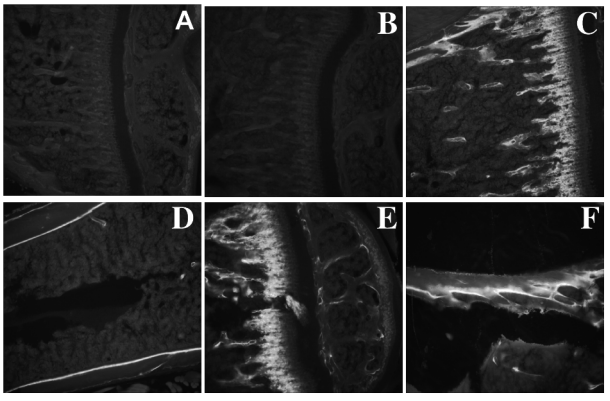

Figure 3. *In vivo* bone binding of HPMA co-polymer conjugates. A. Saline, no autofluorescence observed in the bone; B. P-FITC, no FITC label observed in the bone; C. P-alendronate-FITC, epiphyseal plate and metaphyseal funnel labeled with FITC; D. P-alendronate-FITC, endosteum and periosteum of diaphyseal shaft labeled with FITC; E. P-D-Asp8-FITC, primary spongiosa and metaphyseal funnel labeled with FITC; F. P-D-Asp8-FITC, endosteum of diaphyseal shaft labeled with FITC.

affinity of bone-targeted HPMA co-polymer conjugates for hard tissue. One may speculate that this class of bone-specific conjugates will be applicable to deliver bone-related therapeutic agents with enhanced efficacy and reduced side effects.

Acknowledgments

This research was supported in part by NIH Grant EB00251.

References

1. Odgren PR, Martin TJ. Therapeutic approaches to bone diseases. Science 2000; 289:1508-1514.
2. Uludag H, Yang J. Targeting systemically administered proteins to bone by bisphosphonate conjugation. Biotech Prog 2002; 18:604-611.
3. Pierce WM Jr, Waite LC. Bone-targeted carbonic anhydrase inhibitors: effect of a proinhibitor on bone resorption *in vitro*. Proc Soc Exp Biol Med 1987; 186:96-102.
4. Kasugai S, Fujisawa R, Waki Y, Miyamoto K-I, Ohya K. Selective drug delivery system to bone: small peptide (Asp)6 conjugation. J Bone Miner Res 2000; 15:936-943.

P-28

Prostaglandin E2 Administered by Continuous Infusion Causes High Turnover Remodeling-Induced Cancellous Bone Loss and High Turnover Modeling-Induced New Cortical Bone

Q. Zhang[1], X.Y. Tian[1], M. Su[1], R.B. Setterberg[1], W.S.S. Jee[1], R. Cain[2], Q.Q. Zeng[2], J. Hoover[2], Y.L. Ma[2]
[1] Division of Radiobiology, University of Utah School of Medicine, Salt Lake City, UT, USA,
[2] Gene Regulation, Bone and Inflammation Research Division, Lilly Research Laboratories, Eli Lilly & Co., Indianapolis, IN, USA
E-mail: webster.jee@hsc.utah.edu

The effects of prostaglandin E2 (PGE2) given by continuous infusion or by daily subcutaneous (s.c.) injection were analyzed on proximal tibial metaphysis (PTM), tibial shaft (TX), and lumbar vertebral body (LVB) by histomorphometry. Six-month-old intact female rats were treated with 1 or 3 mg PGE2/kg/day via infudisc continuous infusion or daily s.c. injection for 21 days. In the cancellous bone of the PTM and LVB, PGE2 continuous infusion lowered cancellous bone area, decreased trabecular architecture (decreased width and number and increased separation) and increased osteoid and bone formations, bone resorption, bone turnover with changes in bone resorption exceeding bone formation. In contrast, when administered by s.c. injection, PGE2 increased cancellous bone area, trabecular width, osteoid and bone formations, bone resorption and bone turnover with changes in bone formation greater than bone resorption. In addition, PGE2 decreased the resorption period and increased the formation period during bone remodeling. In cortical bone of the TX, PGE2 continuous infusion had no influence on cortical bone or medullary areas, but the treatment increased intracortical porosity, stimulated massive periosteal formation drift partially compensated by endocortical resorption drift (modeling), which resulted in a slightly increased cortical thickness composed mainly of woven and new lamellar bone. In contrast, when administered by s.c. injection, PGE2 increased cortical area and reduced medullary area, increased periosteal and endocortical bone and endocortical osteoid formations. Thus, continuous infusion resulted in no change in cortical area and medullary cavity, but the cortical bone was composed of woven and new lamellar bone from massive periosteal formation drift. The findings of decreased cancellous bone mass and poorer cortical quality (woven bone and new lamellar bone) suggest that continuous infusion treatment may reduce bone strength. These results indicate that continuous infusion is not a valid means of delivery of PGE2 to increase bone mass and strength.